J. Fluid Mech. (2014), *vol.* 750, *pp.* 507–517. © Cambridge University Press 2014
doi:10.1017/jfm.2014.277

Nonlinear resonance in Anaconda

Chiang C. Mei†

Department of Civil and Environmental Engineering, Massachusetts Institute of Technology, MA 02139, USA

(Received 14 March 2014; revised 10 May 2014; accepted 15 May 2014; first published online 10 June 2014)

A nonlinear theory is developed for a recent wave energy converter design inspired by the mechanics of animal arteries. The device is a long and hollow rubber tube immersed beneath the sea surface. Excited by passing water waves outside, pressure waves are resonated inside the tube and advance toward the stern to spin a turbine for power production. To account for significant magnification, the classical linear theory of blood vessels is modified. Diffraction is neglected but nonlinearity and wall friction are included. The spatial evolution of harmonic amplitudes is shown to be governed by a dynamical system similar to that in nonlinear optics. The maximum available power flux is predicted as a function of the tube length and other structural parameters. It is hoped that the theory may assist further development of the novel device.

Key words: coastal engineering, waves/free-surface flows, wave–structure interactions

1. Introduction

A novel design for extracting energy from sea waves is being developed in the UK using a submerged rubber tube open at both bow and stern and aligned with the incoming waves (Chaplin *et al.* 2012; Farley, Rainey & Chaplin 2012). Pressured by the passing sea waves outside, waves are generated inside which can activate a turbine at the stern for energy production. The idea stems from the mechanics of blood vessels (McDonald 1974; Pedley 1980; Fung 1996, etc.) where waves propagate due to the distensibility of the wall. Some laboratory experiments have demonstrated the feasibility of the concept as a wave energy converter. Since the tube can wiggle in water if it is moored only at the bow, the design has been christened Anaconda by the inventors.

As in most wave energy converters, high efficiency is achieved by resonance. The classical linearized equation for unforced waves in an artery is

$$\frac{\partial^2 p}{\partial t^2} - \frac{E h_0}{2\rho R_0}\frac{\partial^2 p}{\partial x^2} = 0 \tag{1.1}$$

where p denotes the blood pressure, E the Young's modulus of the tube wall, h_0 the mean wall thickness and R_0 the inner radius of the tube (Fung 1996). A propagating wave of frequency ω must have the wavenumber k_0 and phase speed C_0 given by

$$k_0 = \omega\sqrt{\frac{2\rho R_0}{E h_0}} = \frac{\omega}{C_0}, \qquad C_0 = \sqrt{\frac{E h_0}{2\rho R_0}}. \tag{1.2a,b}$$

† Email address for correspondence: ccmei@mit.edu

It is easily shown that if the external excitation is a progressive wave with matching frequency and wave number, the tube wave can be resonated to large amplitude after a long distance (Farley *et al.* 2012). For a rubber tube of given material with known Young's modulus E, matching with sea waves can be achieved by choosing proper R_0 and h_0.

As usual in resonance physics the response can be very much greater than the forcing. This can be seen by using the linearized relation between the typical radial distension a and the tube pressure $p = Eh_0 a/(R_0^2)$ known for blood vessels (Fung 1996). Since the water wave pressure is $p_W \sim \rho g A$ where A is the local wave amplitude around the tube, the magnification ratio can be estimated as

$$\frac{p_W}{p} \sim \frac{k_0^2 R_0 \rho g A}{2\rho\omega^2 a} = \frac{k_0 R_0}{2}\frac{A}{a}. \tag{1.3}$$

Use has been made of the dispersion relation $\omega^2 = gk$ for deep water waves and $k_0 = k$. As the tube radius is expected to be no more than a few metres, and $k \approx 0.025\ \mathrm{m}^{-1}$ for sea swell of 12 s period, kR_0 is typically small. Wall distention as large as the surrounding water-wave amplitude ($a \sim A$) can therefore be excited by relatively small wave pressure. A nonlinear analysis accounting for the finite deformation of the tube wall is therefore warranted, and is pursued here with the view to aiding future choices of tube material and dimensions, etc.

2. Approximate nonlinear equations

We assume that the tube is constrained in a fixed horizontal position along the x axis in order to minimize the loss of wave energy by radiation. The two ends are kept fixed so that the tube distends in plane strain. In this work we shall only consider the radial deformation of a straight tube, as in the experiments by Chaplin *et al.* (2012). Similar configuration has been used to model blood pulses in animal arteries (see Pedley 1980 and Fung 1996). In particular Yomosa (1987) has extended the classical linear theory to predict weakly nonlinear solitary waves in blood vessels by including convective inertia in the fluid, nonlinear wall elasticity and change of tube wall thickness, as well as wall inertia. For convenience we cite below the same conservation laws, and a constitutive relation valid for Anaconda.

Let the inner tube radius $R(x, t)$ be much greater than the wall thickness $h(x, t)$ but much smaller than the wavelength $2\pi/k$, which is in turn much smaller than the tube length L. To be specific we define the small parameter $\epsilon = A/R_0$, where A is the typical amplitude of water wave, and assume

$$O(kR) = O(h/R) = \epsilon = A/R_0 \ll 1. \tag{2.1}$$

We first show that, for a slender tube in head seas, the external wave pressure p_W is dominated by the incident wave $p_W^I \sim \rho g A$ alone, where g is the gravitational acceleration. In other words, pressures from the radiated wave p_W^R due to tube distention, and from the scattered wave p_W^S due to the tube presence, are quite negligible. Let $a(x, t)$ be the radial deformation, which is assumed to be comparable to A. In terms of the radiation potential, the radial velocity of the wall is

$$\frac{\partial \phi^R}{\partial r} = -\mathrm{i}\omega a, \quad \text{hence } \phi^R \sim -\mathrm{i}\omega a R, \ \text{ on } r = R + h. \tag{2.2}$$

Hence

$$p_W^R \sim -\mathrm{i}\omega\rho\phi^R \sim \rho gkR\,a \sim \rho gA(kR) = (kR)p_W^I \ll p_W^I \tag{2.3}$$

since $kR \ll 1$. A similar consideration shows that the scattering pressure p_W^S is comparably small. Thus p_W is dominated by p_W^I alone. For a large tube or short waves, radiation and scattering must of course be considered.

Let $u(x, t)$ be the area-averaged longitudinal fluid velocity, and let $S(x, t)$ be the cross-sectional area of the tube. Mass conservation of fluid flow inside the tube requires

$$\frac{\partial S}{\partial t} + \frac{\partial (uS)}{\partial x} = 0. \tag{2.4}$$

Let $R(x, t) = R_0 + a(x, t)$, where R_0 is the inner radius of the tube at rest and $a(x, t)$ the local radial distention. Substituting $S = \pi(R_0 + a)^2$ we get

$$\frac{\partial a}{\partial t} + \frac{R_0}{2}\left(1 + \frac{a}{R_0}\right)\frac{\partial u}{\partial x} + u\frac{\partial a}{\partial x} = 0. \tag{2.5}$$

Balance of fluid momentum in the longitudinal direction requires

$$\frac{\partial u}{\partial t} + u\frac{\partial u}{\partial x} + \frac{1}{\rho}\frac{\partial p}{\partial x} = -\frac{2\pi R}{\pi R^2}\frac{\tau_w}{\rho} = -\frac{2\tau_w}{\rho R}, \tag{2.6}$$

where p is the water pressure in the tube and τ_w is the wall shear stress.

To simulate solitary waves in micro-vessels in dogs, Yomosa (1987) included inertia in Newton's law for the tube wall. Due to the slenderness of Anaconda, wall inertia is $O(k^2R^2(h/R))$ times the magnitude of the pressure and the hoop stress. Ignoring the inertia term, balance of radial forces on a small angular sector $R\mathrm{d}\theta$ of the tube requires

$$(p - p_W)R\mathrm{d}\theta = 2h\sigma_T\frac{\mathrm{d}\theta}{2}. \tag{2.7}$$

The right-hand side is the total radial component of the hoop stress σ at the two edges of the slice where $h(x, t)$ is the local wall thickness. Assuming linear elasticity and plane strain

$$\sigma_T = \frac{E}{1 - \nu_e^2}\frac{a}{R_0} \tag{2.8}$$

where ν_e is the Poisson ratio. Mass conservation further requires

$$Rh = R_0 h_0, \quad \text{implying } h = \frac{h_0}{1 + a/R_0}. \tag{2.9}$$

Using (2.8) with $\nu_e = 1/2$ and (2.9), (2.7) becomes

$$p - p_W = \frac{4Eh_0}{3}\frac{a}{R_0^2}\left(1 + \frac{a}{R_0}\right)^{-2}. \tag{2.10}$$

Due to (2.9) this relation is nonlinear despite the assumption of linear Hooke's law. For modelling large blood vessels, Yomosa (1987) added a nonlinear term for the hoop stress σ_T and used data for the thoracic aorta of a dog to estimate the new elastic coefficient. For Anaconda such a coefficient would of course depend on the wall material used. Our choice of (2.8) conforms with the experimentally verified relation of Chaplin *et al.* (2012) for a reinforced rubber tube, that is,

$$p-p_W=\frac{4Eh_0}{3R_0}\frac{r'-1}{r'(r'-1+\alpha)}, \tag{2.11}$$

where $r'=R/R_0$ and $\alpha\leqslant 1$ is an empirical factor representing the fraction of rubber used. Equation (2.12) is the limit of (2.11) for $\alpha=1$ for pure rubber. For small a/R_0 we have approximately

$$p-p_W=2\rho C^2\frac{a}{R_0}\left[1-2\frac{a}{R_0}+O\left(\frac{a}{R_0}\right)^2\right], \quad \text{where } C^2=\frac{2}{3}\frac{Eh_0}{\rho R_0}. \tag{2.12}$$

Other nonlinear relations between the pressure difference and the cross-sectional area have been introduced for blood vessels by Olsen & Shapiro (1967) and Anliker, Rockwell & Ogden (1971). For small strains, approximations similar to (2.12) can be obtained from their empirical formulas.

3. Dimensionless nonlinear equations

Let us first define the dimensionless coordinates distinguished by primes: $x'=kx$, $t'=\omega t$, where $k=\omega/C$ is the characteristic wavenumber of the tube and C is defined by (2.12). Since our focus is on resonance, the wavenumber of the surrounding sea waves is also close to k. Relations between characteristic scales of all physical quantities can be found by balancing the linear terms in the governing equations. Using square brackets to denote the scales we find from fluid momentum equation (2.6), and fluid mass,

$$[u]=\frac{\omega}{kR_0}[a]=C\frac{[a]}{R_0}, \quad [p]=\rho\frac{\omega}{k}[u]=\rho C^2\frac{[a]}{R_0}, \quad [p_W]=\rho g[a], \quad [\tau_w]=\frac{\rho\nu}{\delta}[u]. \tag{3.1a–d}$$

The scale of the wall stress is dictated by the classical Stokes theory of oscillatory boundary layers where $\delta=\sqrt{2\nu/\omega}$ is the boundary layer thickness. For convenience we choose $[a]=A$ from here on so that $[a]/R_0=\epsilon\ll 1$.

With these scales we get the normalized equations, distinguished by primes,

$$\frac{\partial u'}{\partial t'}+\epsilon u'\frac{\partial u'}{\partial x'}+\frac{\partial p'}{\partial x'}=-2\frac{[\tau_w]}{\rho R_0\omega[u]}\tau_w'=-\frac{\delta}{R_0}\tau_w', \tag{3.2}$$

$$\frac{\partial a'}{\partial t'}+\frac{1}{2}\left(1+\epsilon a'\right)\frac{\partial u'}{\partial x'}+\epsilon u'\frac{\partial a'}{\partial x'}=0 \tag{3.3}$$

and

$$p'-(kR_0)p_W'=2a'(1-2\epsilon a'). \tag{3.4}$$

We shall assume

$$kR_0=\beta\epsilon, \quad \frac{\delta}{R_0}=\frac{[a]}{R_0}\frac{\delta}{[a]}=\epsilon\gamma, \quad \gamma=\frac{\delta}{[a]}, \tag{3.5a–c}$$

where β and γ are at most of order unity.

By cross-differentiation we first eliminate p and u to leading order, and get

$$\frac{\partial^2 a'}{\partial x'^2} - \frac{\partial^2 a'}{\partial t'^2} = \epsilon \left\{ 2\frac{\partial^2 a'^2}{\partial x'^2} + \frac{1}{2}\frac{\partial}{\partial t'}\left(a'\frac{\partial u'}{\partial x'}\right) + \frac{\partial}{\partial t'}\left(u'\frac{\partial a'}{\partial x'}\right) - \frac{1}{2}\frac{\partial}{\partial x'}\left(u'\frac{\partial u'}{\partial x'}\right) \right.$$
$$\left. - \frac{1}{2}\gamma\frac{\partial \tau_w'}{\partial x'} - \frac{1}{2}\beta\frac{\partial^2 p_W'}{\partial x'^2}\right\}. \tag{3.6}$$

Accurate up to $O(\epsilon)$, the linear approximations of (3.3), (3.2) and (3.4) can be used in all quadratic terms, yielding

$$\frac{\partial^2 a'}{\partial x'^2} - \frac{\partial^2 a'}{\partial t'^2} = \epsilon \left\{ 2\frac{\partial^2 a'^2}{\partial x'^2} - \frac{1}{2}\frac{\partial^2 a'^2}{\partial t'^2} + 2\left(\frac{\partial a'}{\partial t'}\right)^2 - 2\left(\frac{\partial a'}{\partial x'}\right)^2 \right\}$$
$$- \epsilon\left\{\frac{1}{2}\gamma\frac{\partial \tau_w'}{\partial x'} - \frac{1}{2}\beta\frac{\partial^2 p_W'}{\partial x'^2}\right\}. \tag{3.7}$$

From here on, primes will be omitted for all dimensionless variables for the sake of brevity.

4. Resonant evolution in a long tube

Anticipating resonant growth along the tube we introduce the slow coordinate $X = \epsilon x$ and the two-scale expansion:

$$a = a_0(x, t; X) + \epsilon a_1(x, t; X) + \epsilon^2 a_2(x, t; X) + \cdots . \tag{4.1}$$

The perturbation equations are:

$$\frac{\partial^2 a_0}{\partial x^2} - \frac{\partial^2 a_0}{\partial t^2} = 0, \tag{4.2}$$

$$\frac{\partial^2 a_1}{\partial x^2} - \frac{\partial^2 a_1}{\partial t^2} + 2\frac{\partial^2 a_0}{\partial x \partial X} = 2\frac{\partial^2 a_0^2}{\partial x^2} - \frac{1}{2}\frac{\partial^2 a_0^2}{\partial t^2} - \frac{1}{2}\frac{\partial^2 u_0^2}{\partial x^2} + 2\left(\frac{\partial a_0}{\partial t}\right)^2 - 2\left(\frac{\partial a_0}{\partial x}\right)^2$$
$$- \gamma\frac{\partial \tau_w}{\partial x} - \frac{1}{2}\beta\frac{\partial^2 p_W}{\partial x^2}. \tag{4.3}$$

We now assume that the water wave outside is simple harmonic with a slight detuning from the tube wave by ϵK:

$$\beta p_W = \beta e^{iKX} e^{i\theta} + \text{c.c.}, \quad \text{where } \theta \equiv x - t. \tag{4.4}$$

Due to nonlinearity, higher harmonics are expected

$$a_0 = \sum_{\substack{\ell=-\infty \\ \neq 0}}^{\infty} A_\ell e^{i\ell\theta}, \quad u_0 = \sum_{\substack{\ell=-\infty \\ \neq 0}}^{\infty} U_\ell e^{i\ell\theta}, \quad p_0 = \sum_{\substack{\ell=-\infty \\ \neq 0}}^{\infty} P_\ell e^{i\ell\theta}, \tag{4.5a–c}$$

where A_ℓ, U_ℓ, P_ℓ depend on X with $A_0 = U_0 = P_0 = 0$. From the leading order parts of (3.2), (3.3) and (3.4), the first-order harmonic amplitudes are simply related by

$$P_\ell = U_\ell = 2A_\ell. \tag{4.6}$$

In a study of long sea waves in a narrow bay, Rogers & Mei (1987) have shown that

$$a_0^2 = \left(\sum_{\substack{\ell=-\infty \\ \neq 0}}^{\infty} A_\ell e^{i\ell\theta}\right)^2 = \sum_{\substack{m=-\infty \\ \neq 0}}^{\infty} e^{im\theta} \left\{ \sum_{\ell=1}^{[m/2]} \alpha_\ell A_\ell A_{m-\ell} + \sum_{\ell=1}^{\infty} 2A_\ell^* A_{m+\ell} \right\}$$
$$+2\sum_{\ell=1}^{\infty} |A_\ell|^2; \quad \alpha_\ell = 1, \text{ if } \ell = \frac{m}{2}; \quad \alpha_\ell = 2, \text{ otherwise.} \tag{4.7}$$

where $[m/2]$ denotes the integral part of $m/2$. (See also Mei, Stiassnie & Yue (2005) for proof.) The last series in (4.7) is the zeroth harmonic. Since $\partial/\partial x = -\partial/\partial t$ on the right-hand side, the last two terms in the second line of (4.3) cancel. The remaining nonlinear terms add up to

$$-\frac{1}{2}\frac{\partial^2 a_0^2}{\partial x^2} = -\frac{1}{2}\frac{\partial^2}{\partial x^2}\left(\sum_{\substack{\ell=-\infty \\ \neq 0}}^{\infty} A_\ell e^{i\ell\theta}\right)^2. \tag{4.8}$$

We must now choose a model for the wall shear stress. It is known from experiments for oscillatory flows in a smooth pipe that transition to turbulence occurs when $Re_\delta = U\delta/\nu = 550$ (Li 1954 and Hino, Sawamoto & Takasu 1976). Under progressive waves the threshold is lower ($Re_\delta = 160$, Collins 1963). For rough walls such as the seabed, semi-empirical models of turbulent boundary layer in waves have been advanced by Kajiura (1968) and Grant & Madsen (1979) based on the mixing length concept. The prediction depends on the judicious estimate of the wall roughness. Laboratory measurements for walls roughened by sand grains or artificial grooves have shown that the eddy viscosity can be as high as 20–40 $\text{cm}^2\ \text{s}^{-1}$ or $O(10^3)$ that of the molecular viscosity of water (Jonsson 1966). Uncertain of the roughness of future Anaconda we shall adopt the simple model of constant eddy viscosity and estimate its value to be $O(100)$ times that of the molecular viscosity.

Following Stokes theory of monochromatic oscillatory flows near a wall, it can be shown that the velocity in the boundary layer is, in dimensional form

$$u(x, X, r, t) = \sum_{\substack{m=-\infty \\ \neq 0}}^{\infty} [u] U_m(X) \left[1 - \exp\left(-(1 \mp i)\sqrt{|m|}\frac{R_0 - r}{\delta}\right)\right] e^{im(kx-\omega t)},$$
$$\text{if } \begin{cases} m > 0, \\ m < 0, \end{cases} \quad 0 \leqslant \frac{R_0 - r}{\delta} < \infty, \tag{4.9}$$

where U_m is the dimensionless velocity amplitude slowly varying in x, and $\delta = \sqrt{2\nu/\omega}$ is defined by the eddy viscosity ν. The physical shear stress on the tube wall is

$$\tau_w = \rho\nu \left.\frac{\partial u}{\partial r}\right|_{r=R_0} = -\sum_{\substack{m=-\infty \\ \neq 0}} (1 \mp i)\frac{\rho\nu}{\delta}\sqrt{|m|}[u]U_m \, e^{imkx - im\omega t}. \tag{4.10}$$

Since $\tau_w = [\tau_w]\tau_w' = (\rho\nu/\delta)[u]\tau_w'$, the dimensionless shear stress is

$$\tau_w' = -\sum_{\substack{m=-\infty \\ \neq 0}} (1 \mp i)\sqrt{|m|} 2A_m e^{im(x'-t')}, \tag{4.11}$$

after using (4.6).

With these results, (4.3) becomes, after omitting primes,

$$\begin{aligned}\frac{\partial^2 a_1}{\partial x^2}-\frac{\partial^2 a_1}{\partial t^2} &= -2\sum_{\substack{m=-\infty\\ \neq 0}} \mathrm{i}m\frac{\partial A_m}{\partial X}\mathrm{e}^{\mathrm{i}m\theta} \\ &\quad -\frac{1}{2}\frac{\partial^2}{\partial t^2}\sum_{\substack{m=-\infty\\ \neq 0}}^{\infty}\mathrm{e}^{\mathrm{i}m\theta}\left\{\sum_{\ell=1}^{[m/2]}\alpha_\ell A_\ell A_{m-\ell}+2\sum_{\ell=1}^{\infty}A_\ell^* A_{m+\ell}\right\} \\ &\quad +\frac{\beta \mathrm{e}^{\mathrm{i}KX}}{2}\left(\mathrm{e}^{\mathrm{i}\theta}+\text{c.c.}\right)-\gamma\sum_{\substack{m=-\infty\\ \neq 0}}\mathrm{i}(1\mp \mathrm{i})\sqrt{|m|}m[2A_m\mathrm{e}^{\mathrm{i}m\theta}]. \end{aligned} \tag{4.12}$$

Since $\mathrm{e}^{\mathrm{i}m\theta}$ is a homogeneous solution of the wave equation on the left-hand side, the sum of all terms proportional to $\mathrm{e}^{\mathrm{i}m\theta}$ on the right must be set to zero for a_1 to be bounded in the fast-scale coordinates x, t, hence,

$$\frac{\partial A_m}{\partial X}=-\frac{\mathrm{i}}{4}m\left\{\sum_{\ell=1}^{[m/2]}\alpha_\ell A_\ell A_{m-\ell}+2\sum_{\ell=1}^{\infty}A_\ell^* A_{m+\ell}\right\}-(1-\mathrm{i})\sqrt{m}\gamma A_m-\frac{\mathrm{i}\beta}{4}\mathrm{e}^{\mathrm{i}KX}\,\delta_{m1}. \tag{4.13}$$

This is the dynamical system coupling the nonlinear evolution of the harmonic amplitudes. As the sea-wave pressure at the entrance is $O(kR_0)$ times smaller, the initial conditions are:

$$A_m(0)=0,\qquad m=1, 2, 3, 4, \ldots. \tag{4.14}$$

Except for the forcing term proportional to β, this system is of the same form as that governing long waves in shallow sea over a randomly rough seabed (Grataloup & Mei 2003; see also Mei & Ünlüata 1973 and Bryant 1983). Similar equations appeared first in the theory of nonlinear optics (Armstrong *et al.* 1962).

For numerical computation the infinite series is truncated after n terms where n is large. Adding the product of A_m^* with (4.13) and its complex conjugate, and summing over all $m=1, 2, 3, \ldots, n$, we get

$$\begin{aligned}\frac{\mathrm{d}}{\mathrm{d}X}\sum_{m=1}^{n}|A_m|^2 &= -2\gamma\sum_{m=1}^{n}\sqrt{m}|A_m|^2+\operatorname{Im}\left(\frac{\beta}{2}\mathrm{e}^{\mathrm{i}KX}A_1^*\right) \\ &\quad +\frac{1}{2}\operatorname{Im}\sum_{m=1}^{n}m\left[\sum_{\ell=1}^{[m/2]}\alpha_\ell A_\ell A_{m-\ell}A_m^*+2\sum_{\ell=1}^{n-m}A_\ell^* A_{m+\ell}A_m^*\right]. \end{aligned} \tag{4.15}$$

On the right-hand side, the first term represents the energy loss due to wall friction, and the second term is the input due to work done by the wave pressure along the tube. By mathematical induction the remaining series is known to vanish for all n (Grataloup & Mei 2003), implying that nonlinear interactions do not change the total energy.

5. Maximum power-capture width

In terms of the normalized p_0 and u_0 defined in (4.5*a–c*), the dimensional time-averaged power flux $\mathcal{E}$ at the station X is

$$\mathcal{E}(X)=\pi R_0^2[p][u]\int_0^{2\pi}p_0u_0\,\mathrm{d}t=2\pi R_0^2[p][u]\sum_{m=1}^{\infty}A_\ell(X)A_\ell^*(X), \tag{5.1}$$

https://doi.org/10.1017/jfm.2014.277 Published online by Cambridge University Press

since $p_0u_0 = 4a_0^2$ in view of (4.6) and

$$\int_0^{2\pi} 4a_0^2 \, \mathrm{d}t = 2\sum_{m=1}^{\infty} A_\ell(X)A_\ell^*(X). \tag{5.2}$$

If an energy converter such as a Wells' turbine is installed at X, the maximum power available for extraction is $\mathcal{E}(X)$. Recalling the scale relationship (3.1*a–d*), the factor above is

$$\pi R_0^2[p][u] = \pi R^2 \rho \frac{\omega^2[a]}{k^2R_0}\frac{\omega[a]}{kR_0} = \pi\rho\frac{\omega^3}{k^3}[a]^2. \tag{5.3}$$

Assuming plane incident waves in deep water, the rate of energy flux per unit length of the incident wave crest is $EC_g = ((\rho g[a]^2)/2)(\omega/(2k))$. As a measure of the power extraction potential, we define the capture width W by the ratio of the energy extractable to the incident energy per unit length of the incoming wave:

$$kW = \frac{k\mathcal{E}}{EC_g} = 8\pi\sum_{\ell=1}^{\infty}|A_\ell|^2. \tag{5.4}$$

6. Numerical examples

The magnitude of the wall friction depends on the flow rate and the wall roughness both of which affect the magnitude of the model eddy viscosity ν and the factor γ. For reference let us first take the molecular viscosity of water $\nu = 10^{-2}$ cm^2 s^{-1}, then for $\omega = 2\pi/12$ rad s^{-1}, $\delta = 0.2$ cm. For $[a] = 10$ cm, $\gamma = \delta/[a] = 0.02$. We shall take $\gamma = 0.1$ and 0.2 for simulating a turbulent boundary layer. In all computations, eleven harmonics are used and $\beta = 1$.

First, figure 1(*a–d*) shows the first few harmonic amplitudes for four different phase mismatches: $K = 0.0, 0.5, 0.75, 1.0$. The wall friction parameter is fixed at $\gamma = \delta/[a] = 0.1$. For perfect tuning $K = 0$, the first harmonic grows monotonically but slowly, as shown in figure 1(*a*). As detuning increases, the peak amplitudes of all harmonics decrease and the evolution becomes more oscillatory, as seen in figure 1(*b–d*). In light or shallow water waves, energy usually comes from a distant source; harmonic generation is the result of nonlinear interactions. Here energy is constantly supplied along the entire path of propagation. Phase mismatch is the primary cause of envelope oscillations, as can be seen in the limiting case of weak nonlinearity. By letting $A_1 \gg A_m,\ \ m = 2, 3, 4, \ldots,$ the linearized problem for A_1 has the solution

$$A_1 = \frac{\mathrm{i}\beta}{4}\frac{1}{\mathrm{i}K + (1-\mathrm{i})\gamma}(\mathrm{e}^{-(1-\mathrm{i})\gamma X} - \mathrm{e}^{\mathrm{i}KX}). \tag{6.1}$$

When $\gamma X \gg 1$,

$$A_1 \to -\frac{\mathrm{i}\beta}{4}\frac{\mathrm{e}^{\mathrm{i}KX}}{\mathrm{i}K + (1-\mathrm{i})\gamma}, \tag{6.2}$$

hence $|A_1|$ is monotonic in X if there is no phase mismatch ($K = 0$), and oscillatory otherwise. If the wall friction is greater, the peak amplitudes of all harmonics are lower, and are attained within a shorter distance.

If the power take-off device at the stern is perfectly efficient, the maximum power available to a tube of total length X is given by (5.1). In figure 2(*a*,*b*), we compare the maximum capture width of two tubes with different wall friction. For either tube,

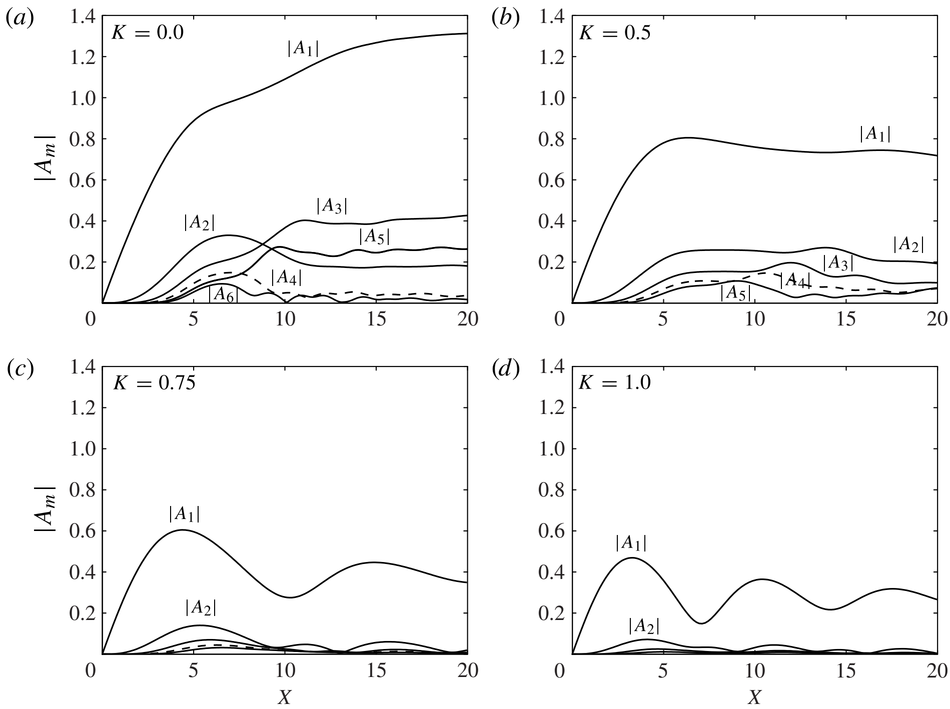

FIGURE 1. Evolution of harmonics. $\gamma = 0.1$.

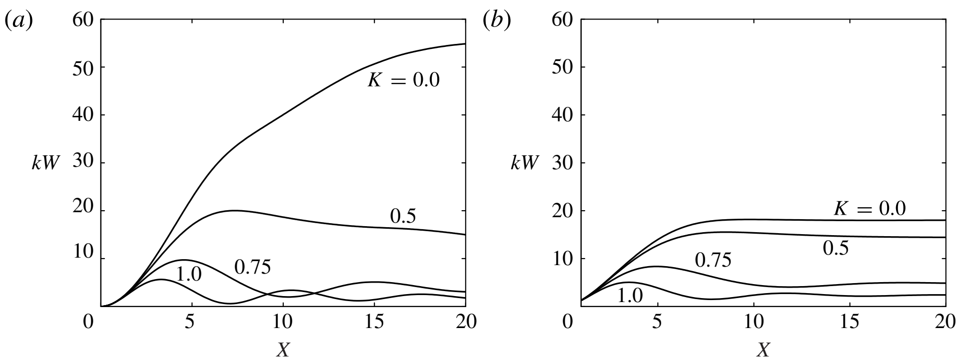

FIGURE 2. Maximum capture width. (*a*) $\gamma = 0.1$, (*b*) $\gamma = 0.2$.

perfect phase matching yields the highest power output. Potential productivity is reduced if the mismatch is greater. Since larger detuning makes the energy flux more oscillatory, fluctuations of power extractable must be expected from a tube of fixed length, due to variations of wave spectrum. Not surprisingly, the tube with less wall friction gives greater output.

It is known that an isolated buoy absorbing energy from heave only has the maximum capture width $kW_{max} = 1$. This is achieved in a typical swell only if the buoy is sufficiently large. For an elongated raft, where energy is absorbed from connecting hinges, the optimal capture width is comparable to the wavelength if it is comparable to the total raft length (Newman 1979). In comparison, the best efficiency for Anaconda is achieved around $X = \epsilon kx = O(1)$, hence the tube must be many wavelengths long. But the dimensionless capture width kW can be considerably greater than unity.

Experiments for testing the predictions here would be very worthwhile. Further improvement of the fluid-mechanical theory is desirable to assist the development of Anaconda. To account for head-sea diffraction by a tube of moderately large radius, and the accompanying radiation due to tube distention, a theory similar to that by Haren & Mei (1981) for a raft-like converter appears possible. Since power take-off devices such as turbines are likely imperfect, wave reflection inside the tube and radiation from the bow may need to be examined. Of course other factors such as the costs of materials, construction, maintenance and operation must also be weighed for its realization as a contributor to renewable energy.

Acknowledgements

I thank Professors F. Farley, FRS, J. Chaplin and R. Rainey of the University of Southampton for information about Anaconda.

REFERENCES

Anliker, M., Rockwell, R. L. & Ogden, E. 1971 Nonlinear analysis of flow pulses and shock waves in arteries. *Z. Angew. Math. Phys.* **22**, 217–246.

Armstrong, J. A., Bloembergen, N., Ducuing, J. & Pershan, P. S. 1962 Interaction between light waves in a nonlinear dielectric. *Phys. Rev.* **127**, 1918–1939.

Bryant, P. J. 1983 Periodic waves in shallow water. *J. Fluid Mech.* **59**, 624–644.

Chaplin, J. R., Heller, V., Farley, F. J. M. & Hearn, G. E. 2012 Laboratory testing the Anaconda. *Phil. Trans. R. Soc. Lond.* **370**, 403–424.

Collins, J. I. 1963 Inception of turbulence at the bed under periodic gravity waves. *J. Geophys. Res.* **18**, 6007–6014.

Farley, F. J. M., Rainey, R. C. T. & Chaplin, J. R. 2012 Rubber tubes in the sea. *Phil. Trans. R. Soc. Lond.* **370**, 381–402.

Fung, Y. C. 1996 *Biomechanics: Circulation*. Springer.

Grant, W. H. & Madsen, O. S. 1979 Combined wave and current interaction with rough bottom. *J. Geophys. Res.* **84**, 1797–1808.

Grataloup, G. & Mei, C. C. 2003 Localization of harmonics generated in nonlinear shallow water waves. *Phys. Rev.* E **68**, 026314.

Haren, P. & Mei, C. C. 1981 Head-sea diffraction by a slender raft with application to wave-power absorption. *J. Fluid Mech.* **104**, 505–526.

Hino, M., Sawamoto, M. & Takasu, S. 1976 Experiments on transition to turbulence in an oscillatory pipe flow. *J. Fluid Mech.* **75**, 193–207.

Jonsson, I. G. 1966 Wave boundary layers and friction factors. In *Proceedings of 10th Conference Coastal Eng. ASCE*, pp. 127–148.

Kajiura, K. 1968 A model of the bottom boundary layer in water waves. *Bull. Earthq. Res. Inst., Univ. Tokyo* **46**, 75–123.

Li, H. 1954 Stability of an oscillatory laminar flow along a wall. US Army, Beach Erosion Board Tech. Memo. 47.

McDonald, D. A. 1974 *Blood Flow in Arteries*. Edward Arnold.

Mei, C. C., Stiassnie, M. & Yue, D. K.-P. 2005 *Theory and Applications for Ocean Surface Waves*. vol. II. World Scientific.

Mei, C. .C. & Ünlüata, Ü. 1973 Harmonic generation in shallow water waves. In *Waves on Beaches* (ed. R. E. Meyer), pp. 181–202. Academic Press.

NEWMAN, J. N. 1979 Absorption of wave energy by elongated bodies. *Appl. Ocean Res.* **1**, 189–196.

OLSEN, J. H. & SHAPIRO, A. H. 1967 Large-amplitude unsteady flow in liquid-filled elastic tubes. *J. Fluid Mech.* **29**, 513–538.

PEDLEY, T. M. 1980 *The Fluid Mechanics of Large Blood Vessels*. Cambridge University Press.

ROGERS, S. R. & MEI, C. C. 1987 Nonlinear resonant excitation of a long and narrow bay. *J. Fluid Mech.* **88**, 463–479.

YOMOSA, S. 1987 Solitary waves in large blood vessels. *J. Phys. Soc. Japan* **56** (2), 506–520.